International Journal of Innovative Research in Engineering & Management (IJIREM)
ISSN: 2350-0557, Volume-2, Issue-6, November- 2015

Enhanced As(V) Adsorption Properties in Sn-Substituted Goethites - Changes in Chemical Reactivity and Surface Characteristics

Ana L. Larralde
INQUIMAE, DQIAQF, FCEN – Universidad de Buenos Aires. Int. Güiraldes 2160, Pab. 2, Piso 3 C1428EHA, Bs. As., Argentina.
alarralde@qi.fcen.uba.ar

Ana E. Tufo
Laboratorio de Química Ambiental, 3iA –ECyT, UNSAM, Buenos Aires, Argentina.
anatufo@qi.fcen.uba.ar

Pedro J. Morando
Unidad de Actividad Química, CAC, CNEA, Inst. de Tecnología J. Sábato, UNSAM, Av. Gral. Paz 1499, 1650, San Martín, Bs. As., Argentina
morando@cnea.gov.ar

Elsa E. Sileo
INQUIMAE, DQIAQF, FCEN – Universidad de Buenos Aires. Int. Güiraldes 2160, Pab. 2, Piso 3 C1428EHA, Bs. As., Argentina
Tel. +5411 45763380
sileo@qi.fcen.uba.ar

ABSTRACT
In this work, the adsorption of arsenic (V) onto crystalline substituted goethites was studied for samples with different Sn-contents. The highest Sn-content of the prepared samples was 5.5 (expressed as 100×[Sn]/[Sn]+[Fe]) as all attempts to prepare goethites with higher tin content only rendered amorphous materials. The Sn-for-Fe substitution caused changes on the physico-chemical properties of the obtained samples, and the thermal analysis indicated that the formed Sn-goethites were metal-deficient goethites with increased thermal stabilization towards decomposition to hematite. BET surface analysis evidenced the presence of large mesoporous or macroporous in all samples and the following trend in SSA values: GSn5.5 (54.90±0.08) > GSn0 (25.75±0.09) > GSn2.1 (17.19±0.05 m^2g^{-1}). The As(V) adsorption presented a maximum at pH = 5.50 ± 0.05 for all samples and the data showed that GSn5.5 nearly duplicates the amount of As adsorbed per gram of pure goethite. To evaluate the chemical stability of the samples, dissolution kinetics measurements in acidic conditions were also performed. Dissolution rate followed the trend GSn2.1 > GSn0 > GSn5.5. The facts that GSn5.5 dissolves slower than the pure sample and that adsorbs twice as much as pure goethite indicate that GSn5.5 is a promising agent for As(V) removal technologies.

Keywords
Arsenic; Sn-goethite; adsorption, thermal stability; specific surface area; dissolution.

1. INTRODUCTION
Both goethite and ferrihydrite are commonly found in soils, exhibit a highly reactive surface and a strong affinity for As(V) and As(III) [1,2]. Besides, both oxides highly influence the mobility behavior of As [3] in natural environments. In particular, goethite (α-FeOOH), is one of the thermodynamically most stable iron oxide at ambient temperature, and the mineral often forms through the weathering of iron-rich minerals [4]. The oxide has been used since prehistoric times as a natural pigment and also serves as a catalyst of various reactions [5–10] and because of its affinity for many ions can be used to adsorb pollutant ions in water chemistry plants [11]. As the metal substitution in Fe (hydr)oxides results in changes in crystal size, surface charge and surface area, the incorporation of foreign metals also alters their adsorption of ions and molecules. For instance, Masue et al. [12] have demonstrated that As(III) and As(V) adsorption onto several Al-Fe hydroxides decreases as the Al:Fe molar ratio increases. Silva et al. [13] have tested the potential of several Al-goethites (specific surface areas, SSA; in the range 124.7-113.2 m^2g^{-1}) in adsorbing As(V) and found that the presence of structural Al in the goethites enhanced considerably the As uptake when compared to pure goethite (SSA 20.6 m^2g^{-1}). Also the incorporation of Pb(IV) in goethite has proven to increase the adsorption capacity for As(V) [14], and the removal of As(V) by Cu(II)-, Ni(II)-, and Co(II)-doped goethite has shown to follow the order Cu(II)-doped goethite ≥ Ni(II)-doped goethite > Co(II)-doped goethite > pure goethite [15].

Incorporation in synthetic goethite is easily achieved and several elements have been incorporated into its structural framework. Metal-for-Fe substitution in goethite have been reported among others for chromium [16–19], cobalt [20,21], manganese [22–26], cadmium [27–29], vanadium [30], nickel, copper, zinc, and lead [31]. Multi-metal substitution has also been reported [32–34].

In particular, Berry et al. [35] have prepared Sn(IV)-doped goethites from Sn(II) and Fe(III) solutions using aqueous ammonia and an hydrothermal process at 200 ºC and 15 atm pressure but the spatial characteristics of the obtained Sn-goethites were not reported because the X-ray powder diffraction data of their samples was not amenable to refine to a structural model. In our laboratory we succeeded in obtaining crystalline tin-doped goethites using milder conditions and a more inexpensive preparative method [36]. The samples were obtained by the aging of basic solutions of Sn(II) and Fe(III) at 70ºC for 20 days, at atmospheric pressure. The final Sn-content of the prepared samples (μ_{Sn}) was 2.1±0.1 and 5.5±0.1 mol mol^{-1} (μ_{Sn}=[Sn]×100/[Sn]+[Fe], [Me]: mol L^{-1}) when the initial Sn concentrations were 5.00 and 10.00 mol mol^{-1} respectively, and all attempts to synthesize goethites with higher tin content have failed as the preparations rendered amorphous materials. The solids were highly crystalline and the Rietveld refinement of XRD data showed that Sn partially substituted the Fe(III) ions provoking unit cell expansion and an average polyhedron

distortion that enlarged the intermetallic distances. The refinement also indicated that Sn-incorporation increased the crystallinity of the particles with enlarged domains that grow in the perpendicular and parallel directions to the anisotropic broadening (111) axis. Morphological observations by SEM measurements demonstrated that the shape of the particles was modified by the Sn-incorporation with a length to width ratio that decreased with the Sn content. Using ^{119}Sn and ^{57}Fe Mössbauer spectroscopy we have also shown that Sn(II) is incorporated as Sn(IV) and that Fe(II) was not present in the samples. It was concluded that the charge balance in tin-doped goethite was achieved by the formation of cation vacancies in the Sn-incorporated samples.

The end product of the thermal dehydroxylation of goethite is hematite. Usually, a typical differential thermogram of goethite presents a smooth loss in the temperature range 30-140 ºC that is due to the release of absorbed water and a well-defined endothermic peak in the range 200-400 ºC which corresponds to the dehydroxylation of the sample to give H_2O and α-Fe_2O_3. A stoichiometric goethite shows a mass loss of 10.13% during its transformation to hematite, however metal-deficient goethites, with OH^-/O^{2-} ratio > 1, present larger mass loss values. The transformation temperature depends on the crystallinity of the sample and on the type and degree of substitution. For instance, Sileo et al. [19] have found that the transformation temperature of a series of Cr-goethites is shifted to higher values when the Cr content increases. The same trend was observed for Al- [37], Mn- [24] and Co-substituted goethites [20].

2. EXPERIMENTAL

2.1 Samples Preparations and Analysis

2.1.1 Adsorbents

Three samples of pure and substituted goethites with a Sn-content of 0.0, 2.1 and 5.5 mol mol^{-1} (expressed as 100×[Sn]/[Sn]+[Fe]) were synthesized and fully characterized following the procedure used by Larralde et al. [36]. Reagent grade chemicals were used. In all experiments, solutions were prepared with high-purity 18 MΩ cm^{-1} water. The samples were named GSn0, GSn2.1 and GSn5.5.

2.1.2 Thermal analysis

Thermogravimetric (TGA) and differential thermal analysis (DTA) were performed in a TGA-51 and a DTA-50 Shimadzu equipment. Samples of about 12.0 mg (for TGA measurements) and 6.0 mg (for DTA measurements) were heated in a N_2 atmosphere in the temperature range 30-450 ºC (heating rate 5 ºC/min).

2.1.3 Specific surface areas (SSA)

The surface areas were determined by physical N_2 adsorption/desorption at 77 K using a Micrometrics ASAP 2020 equipment. The SSA values were derived from N_2 adsorption/desorption isotherms by means of the BET equation [38].

2.2 Acidic Dissolution Experiments

The chemical stability of the samples was measured in magnetically stirred, thermostated double jacket cells with perforated stoppers provided with temperature sensors and sampling port. The dissolution behaviors were tested in 6.0 M HCl at 70.00±0.02 °C. In a typical experiment the reaction was started by adding the oxide (ca. 20 mg) in 100 mL of the mineral acid solution. Approximately 15 aliquots of 1 mL volume each were withdrawn from the suspension during each run using a micropipette. The aliquots were filtered through a 0.22 μm cellulose acetate membrane. All chemicals were analytical grade and the solutions were prepared with high purity 18 MΩ cm^{-1} water. Dissolved iron concentrations were obtained spectrophotometrically using the thioglycolic acid method [39]. All samples achieved total dissolution in the dissolving media and re-precipitation of metals was not detected. These indicated that the reagent concentrations were sufficient to keep metal ions in the form of soluble complexes.

2.2 Adsorption Experiments

2.3.1 Effect of pH on arsenic adsorption

The adsorption capacity of the prepared samples was measured at various pH values (4 to 7), and plotted versus pH to construct the adsorption envelopes. The suspensions were prepared from solids hydrated by thirty minutes sonication before the addition of the sorbates. The experiments were conducted at pH 4.00±0.05, 5.50±0.05, 7.00±0.05 and at 25.00±0.02ºC under a N_2 atmosphere. The thermostated double jacket cells used were magnetically stirred and presented perforated stoppers provided with pH and temperature sensors. The pH values of individual samples were adjusted using an automatic titrator (Mettler T70) by adding 0.1 M KOH or HNO_3. The adsorbents (ca. 200 mg) were placed in contact with arsenate solutions (100 mL, 0.53 mmol L^{-1}) prepared by dissolving analytical grade di-sodium hydrogen arsenate heptahydrate ($Na_2HAsO_4.7H_2O$, Merck) in Milli-Q water. KNO_3 0.1 M was used as background electrolyte for all the experiments. Approximately 15 aliquots of 1 mL volume each were withdrawn from the suspension during each run and syringe-filtered over a 0.22 μm cellulose acetate membrane. Arsenic concentrations were obtained spectrophotometrically using the molybdenum blue method [40].

2.3.2 Effect of Sn-concentration on arsenic adsorption

The adsorption of As(V) was conducted on samples GSn0, GSn2.1 and GSn5.5 as a function of reaction time. The experiments were carried out using a similar procedure detailed in the previous section. The pH values were fixed at 5.50±0.05 for all the samples.

2.4 Electrophoretic Mobility

Electrophoretic mobility (EM) measurements were performed at room temperature using a Brookheaven 90 Plus Particle Size Analyzer. Samples were prepared by adding approximately 3 mg of the solid to 20 mL of 0.01 M KNO_3 solution. The pH value was adjusted in the range 3 to 9 by adding 0.1 M KOH or 0.1 M HNO_3 and three sets of ten points were measured for each sample. The values were expressed as mV.

3. RESULTS AND DISCUSSION

Different techniques were used in the materials characterization to provide information on the physical properties dependence on the composition of the samples.

3.1 Thermogravimetric Analysis

The thermal treatment of goethite in the temperature range 30-200 ºC eliminates adsorbed water, and the measured TGA data

indicated that the adsorbed water in the prepared samples did not exceed 1 wt. %.
At higher temperatures (range 200-400 ºC) dehydroxylation takes place to give hematite and stoichiometric pure goethite presents a mass loss of 10.13% according to the following equation:

$$2\ \alpha\text{-FeO(OH)} \rightarrow \alpha\text{-}Fe_2O_3 + H_2O.$$

However, as in the substituted goethites Fe(III) is replaced by Sn(IV), the expected mass for the stoichiometric (hydr)oxide decreases according to the following expression:

$$2\ \alpha\text{-}(Fe_{1-x}Sn_x)O_{1+x}(OH)_{1-x} \rightarrow \alpha\text{-}(Fe_{1-x}Sn_x)_2O_{3+x} + (1\text{-}x)\ H_2O.$$

When the OH^-/O^{2-} ratio > 1, the mass of the released water is also larger, and the dehydroxilation process can be described by:

$$2\ \alpha\text{-}(Fe_{1-x}Sn_x)_{1-y/3}O_{1+x-y}(OH)_{1-x+y} \rightarrow (1\text{-}y/3)\ \alpha\text{-}(Fe_{1-x}Sn_x)_2O_{3+x} + (1\text{-}x+y)\ H_2O$$

that involves the formation of a metal-deficient goethite with a total metal content of 1-y/3 (y>0). Thus, the experimental mass allows the calculation of the stoichiometry of the synthetized goethites.
The experimental mass losses measured by the TGA measurements and the calculated stoichiometries for the obtained Sn-substituted goethites are shown in Table 1.

Table 1. Thermal analysis data and specific surface area measurements

	GSn0	GSn2.1	GSn5.5
H_2O % released (experimental)	11.72±0.02	11.60±0.02	10.52±0.02
H_2O % released (stoichiometric)	10.13	9.98	9.75
DTA peak (°C)	286.1	296.0	302.0
BET surface area (m^2/g)	25.75±0.09	17.19±0.05	54.90±0.08

All the measured mass losses were larger than that of the stoichiometric values indicating that the OH^-/O^{2-} ratio > 1, and that the stoichiometries of the prepared goethites were α-$Fe_{0.948}O_{0.843}(OH)_{1.157}$ for GSn0, α-$Fe_{0.926}Sn_{0.020}O_{0.837}(OH)_{1.162}$ for GSn2.1 and α-$Fe_{0.920}Sn_{0.054}O_{0.921}(OH)_{1.079}$ for GSn5.5 (all relative errors in the range 0.003-0.004).
The DTA traces for the samples are shown in Figure 1. As can be seen, the endothermic peak, corresponding to the structural water released from the OH^- groups, is displaced to higher temperatures when the Sn content increases, indicating that the incorporation of Sn increases the thermal stability of the goethites

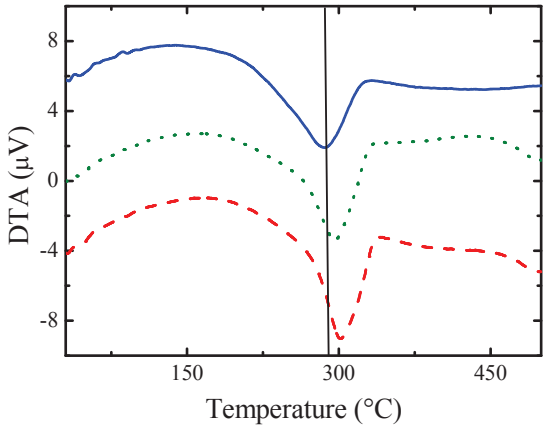

Figure 1. DTA traces for GSn0 (–), GSn2.1 (···) and GSn5.5 (-.-).

3.2 Specific Surface Analysis

The measured N_2 adsorption-desorption isotherms for the three samples are shown in Figure 2. The form and maximum adsorption value of the isotherm varied with the Sn-for-Fe substitution, and in all cases the measured maximum values were low indicating a poor N_2 retention. The three samples presented a rapid increase in N_2 adsorption at p/p° ~ 1, which indicated the presence of large mesoporous or even macropores.
Isotherms for samples GSn0 and GSn2.1 were convex to the p/p° axis over its entire range presenting a weak hysteresis loop at high p/p°. According to the IUPAC classification [41] this feature indicates a Type III isotherm where only a monolayer coverage is achieved.
The shape of the GSn5.5 isotherm differed from the previous ones presenting the hysteresis loop at lower p/p° values. This shape is attributed to both monolayer and multilayer adsorption, and corresponds to a type IV isotherm [41].
The SSA values followed the trend GSn5.5 (54.90±0.08) > GSn0 (25.75±0.09) > GSn2.1 (17.19±0.05 m^2g^{-1}). The data indicated that the most crystalline goethite (GSn5.5) [36] presents the largest specific surface area.

3.3 Dissolution Experiments

In order to determine how the Sn-for-Fe substitution varies the chemical stability of the goethites, dissolution experiments at 70.00 °C in 6.0 M HCl were performed. The results are presented in Figure 3 where the fractions of Fe dissolved, f_{Fe} (f_{Fe} = dissolved Fe mass/total Fe mass) were plotted as function of reaction time. As can be seen the Sn-substituted goethites dissolved more slowly than pure goethite, indicating a stabilization towards mineral acid dissolution with Sn-substitution.

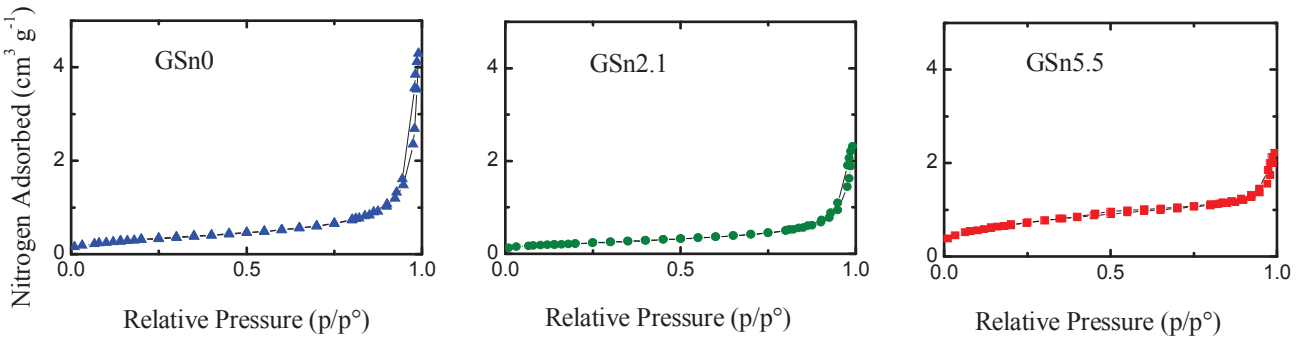

Figure 2. N_2 adsorption – desorption isotherms for samples GSn0 (-▲-), GSn2.1 (-●-) and GSn5.5 (-■-).

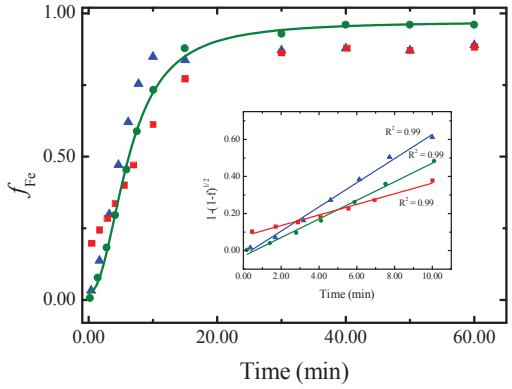

Figure 3. Dissolution-time curves for GSn0 (▲), GSn2.1 (●) and GSn5.5 (■) in HCl 6.0 M and 70.00 ± 0.02 °C. The application of the bidimensional contracting model is shown in the inset. Reported data correspond to average values from three independent dissolution runs.

The three kinetic runs showed a deceleratory behavior. The data were fitted to several kinetic laws, such as the Avrami-Erofejev 2D and 3D model [42], the contracting cylinder model (bidimensional geometry) [43], and the contracting sphere model (three dimensional geometry) [43]. All kinetics laws accurately described the obtained data, however and according to SEM measurements that revealed an elongated form of the goethite particles [36], we inform the parameters obtained by applying the contracting cylinder model. Within this model [44] the rate law expression is obtained on the assumption of an isotropic dissolution where the reaction proceeds inwards at a constant rate at all crystal surfaces, taking the following expression:

$$1 - (1 - f)^{\frac{1}{2}} = kt$$

where k (dissolution rate constant expressed in s^{-1}) represents the advance of the reaction on the surface of the particle.

The dissolution rate constants k, expressed per mol of Fe in the (hydr)oxide, calculated from the initial nearly linear region of the dissolution curves, are presented in Table 2. The calculated rate constants k´, expressed in mol Fe $m^{-2}s^{-1}$, are also shown.

Data in Table 2 indicates that Sn-for-Fe substitution reduces the dissolution rate, and the most substituted sample is the most stable towards dissolution. The release of Fe decreased with Sn-substitution and highly substituted goethites retained Sn more efficiently than α-Sn,FeOOH with a low level of incorporation. In our case, and when expressed per gram of Fe in the oxide, pure goethite dissolved more than two times faster than GSn5.5. This fact is opposite to the results found by Alvarez et al. when studying the reactivity in acid media of Mn-goethites [25], and Co-goethites [20] that reported than in samples with similar degree of substitution the reactivity per gram displayed the following order, Co-goethite > Mn-goethithe > pure goethite. Our results are in line with those of Tufo et al. [45] that found that the reactivity of Cr-substituted goethites in mineral acid media at 70 °C, is lower than the one of pure goethite.

Table 2. Dissolution rate constants and kinetic data for the adsorption of As(V) onto the goethites as affected by the Sn content

Sample	GSn0	GSn2.1	GSn5.5
k (mol Fe g^{-1} s^{-1})	1.19×10^{-5}	8.08×10^{-6}	5.16×10^{-6}
k´ (mol Fe m^{-2} s^{-1})	4.62×10^{-7}	4.70×10^{-7}	0.94×10^{-7}
k_{ads} (g min^{-1} mM^{-1})	1.717±0.150	0.839±0.084	1.897±0.190
k'_{ads} (m^2 min^{-1} mM^{-1})	44.213±3.9	14.422±1.4	104.145±10.4
$[As]_{teq}$ (mM g^{-1})	0.552±0.050	0.924±0.050	1.124±0.050

Dissolution per unit area followed the trend GSn2.1 > GSn0 > GSn5.5, indicating that a small degree of Sn-for-Fe substitution enhances the reactivity per unit area in goethites, and a larger degree of substitution passivates the surface towards mineral acid dissolution. Regarding the k´ value of GSn5.5 (0.94 x 10^{-7} mol Fe m^{-2} s^{-1}), the comparison of these results with the ones of Tufo et al. [45] for a Cr-goethite with similar substitution (μCr = 5.0), they reported a value of k´= 9.14 x 10^{-9} mol Fe m^{-2} s^{-1}. Taking into account that the authors have obtained the rate constants using HCl 3.98 M, whereas we used HCl 6.0 M, the values of the two constants indicate that both, Sn and Cr incorporation, enlarge the stability of substituted goethites, and that the stabilization is larger when Cr is incorporated.

3.4 Adsorption

3.4.1 Effect of pH on arsenic adsorption

The effect of pH on the adsorption of As(V) onto samples GSn0, GSn2.1 and GSn5.5 was studied with an initial concentration of 0.53 mmol L^{-1}, and an equilibration time of 120 min. After equilibration, un-adsorbed arsenic and the final pH of the solution were measured. The results are displayed in Figure 4 and showed a maximum of adsorption at about pH 5.5 in all samples. At this pH value arsenic acid (H_3AsO_4), with pKa values of 3.6, 7.3 and 12.5, predominantly exists as the monovalent anion, $H_2AsO_4^-$. After the maximum, the adsorption of As(V) decreased with the increase of pH as found by other authors for pure goethite [46–48].

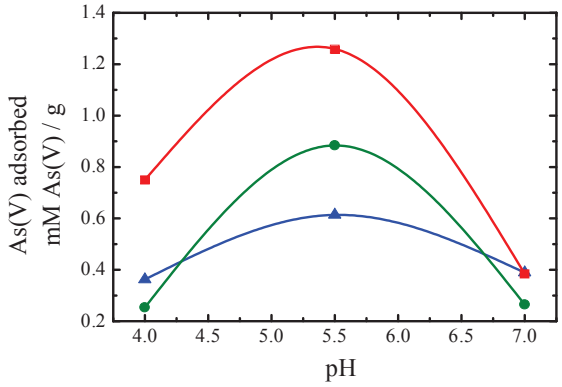

Figure 4. Effect of pH on As(V) adsorption onto samples GSn0 (-▲-), GSn2.1 (-●-) and GSn5.5 (-■-). All symbols are experimental averaged data from several independent measurements.

The shape of the curve indicated that the influence of pH on the adsorption capacity of the sample is higher in the Sn-goethites than in pure goethite.

3.4.2 Effect of Sn-substitution on arsenic adsorption

The experiments of adsorption of As(V) onto the three samples were conducted at pH 5.50±0.05, where the maximum adsorption was detected (see Figure 4), and at 25.00±0.02 ºC using arsenate, $H_xAsO_4^{-3+x}$ (concentration 0.53 mmol L^{-1}). The adsorption method was previously standardized and performed under a N_2 atmosphere. As all the inorganic species (Sn(IV), Fe(III) and As(V)) were fully oxidized, the results in this inert atmosphere will not differ from the ones obtained in an oxidizing environment. The variation of As(V) adsorption with the contact time is shown in Figure 5, where a plateau is reached in less than 30 minutes of observation.

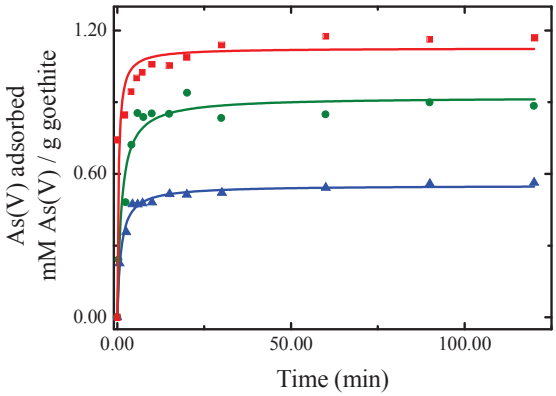

Figure 5. As(V) (mM g^{-1}) adsorbed vs. time for the different goethites: GSn0 (-▲-), GSn2.1 (-●-) and GSn5.5 (-■-). Solid lines correspond to the fitting of the data to the pseudo-second order kinetic rate model. Each adsorption curve is an averaged value from three independent adsorption runs.

The kinetic data was modeled using a pseudo-second order rate equation [49] that has been widely used to describe organic compounds and metal adsorption on different adsorbents [50]. The pseudo-second order kinetic rate equation is expressed as:

$$\frac{t}{[As]_t} = \frac{1}{k_{ads}\,[As]_{t,eq}^2} + \frac{1}{[As]_{t,eq}}\,t$$

where $[As]_{t,eq}$ is the amount of As adsorbed at equilibrium expressed in mM g^{-1}, k_{ads} is the rate constant of adsorption (in g mM^{-1} min^{-1}), and $[As]_t$ is the amount of As adsorbed onto the surface of the solid (in mM g^{-1}) at different contact time, t (in min).

The experimental data followed the equation and straight lines were obtained when $t/[As]_t$ was plotted vs. t, indicating that the process follows the pseudo-second order rate equation. The fit of the experimental data to the second order equation may indicate that the process controlling the rate is a chemical adsorption involving valence forces through sharing or exchange of electrons between adsorbent and adsorbate [51,52].

The results of the fitting (see Table 2) indicated that the Sn-goethites adsorbed more As(V) than the pure one, and that the adsorption on GSn5.5 doubles the one in GSn0 (see values of $[As]_{t,eq}$, and Figure 4). The adsorption rate constants (k_{ads}) values, expressed per gram indicate that the fastest adsorbing sample is GSn5.5, followed by pure goethite, being GSn2.1 the solid with the smallest k_{ads}. A similar trend in rate adsorption is obtained when k_{ads} is expressed per m^2, and the data demonstrate that the affinity of the surface of GSn5.5 for As(V) more than doubles the one of GSn0.

3.5 Electrophoretic Mobility

As researchers have shown that arsenate is specifically adsorbed on iron oxides, such as goethite, forming inner-sphere complexes via a ligand exchange mechanism [53–55], and that the adsorption releases OH^- groups from the adsorbent provoking a shift in the point of zero charge (PZC) of the adsorber, Zeta Potential measurements (ZP) were conducted for all samples before and after the As(V) adsorption experiments, using the electrophoretic mobility (EM) technique. The results are shown in Figure 6.

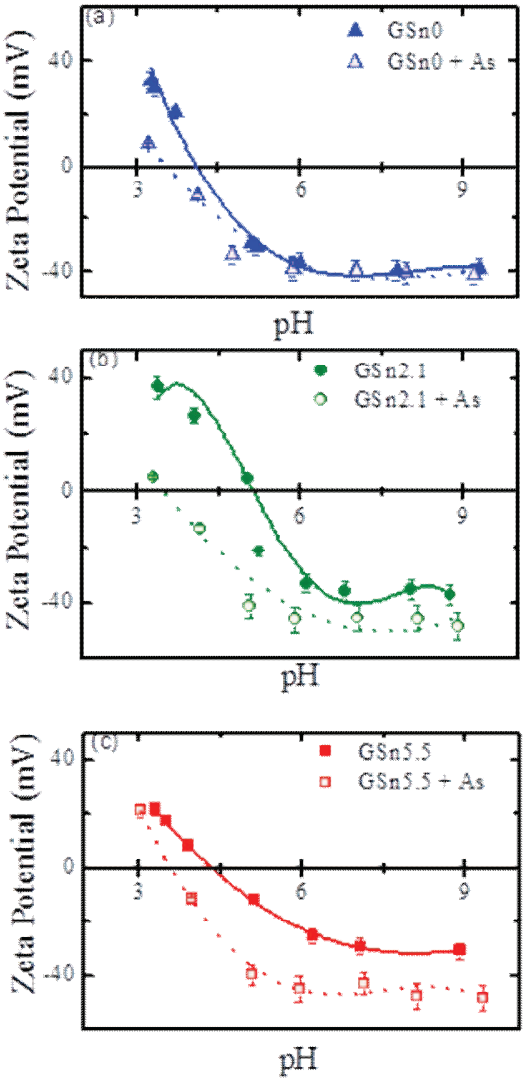

Figure 6. Zeta potential vs. pH measurements and polynomial fitting for the prepared samples before and after As adsorption. ZPC values were calculated from the intersection of the polynomial with the X- axis

Electrophoretic mobility measurements are related to the movement of suspended particles under the influence of an electric field, where the direction of the movement depends on the particles´ charge. The charge of the particles is highly influenced by the pH of the solution, and the pH value on which the oxide particles do not move under the applied electric field is called the point of zero charge (PZC), and the shift may be used as an indirect evidence for adsorption of As(V) on Fe adsorbers [56]. The PZC indicates the ranges in which the surface of the solid is positively or negatively charged. At pH < pH_{PZC} the predominant surface groups are positive ($\equiv FeOH_2^+$), and at pH > pH_{PZC}, are negatively charged ($\equiv FeO^-$).

As can be seen in Figure 6 (a), all ZP values of the As-adsorbed pure goethite are lower than those of the non-adsorbed sample, with PZC decreasing from 4.00 to 3.54. The obtained PZC for pure goethite agrees with the ones obtained for goethites prepared following similar procedures [57], but is lower when compared with other reported values [12,13,58]. Van Schuylenborgh and Arens [59] had ascribed this low PZC to the synthetic procedure where the suspension was aged for several days in a strong basic media that provoked the coprecipitation of OH groups during the slow formation of goethite. The shift in ZPC indicated that the adsorption of arsenate is taking place by ion exchange mechanism where OH^- ions are replaced with arsenate anions, showing a specific adsorption of arsenate on the (hydr)oxide rather than a pure electrostatic interaction.

The effect of the As-adsorption onto the Sn-goethites is displayed in Figures 6 (b) and 6 (c) and revealed varied PZC values for different Sn-incorporations. The finding coincided with data from Vega et. al [60] that reported that the overall surface charge of goethite is affected by the presence of foreign metal ions, and when a partial replacement of Fe(III) by other elements occurs into the structure, a shift in the value of the ZCP with respect to pure goethite may be expected. The non-adsorbed samples showed PZC values at 4.89 and 4.36 for GSn2.1 and GSn5.5, respectively, showing that the surface charge of the samples did not change monotonously with the Sn-incorporation, and that a small incorporation of Sn provokes the exposition of higher sites of actives centers.

In both cases, all ZP were lower in the As-adsorbed samples indicating again the specific adsorption of arsenate on the (hydr)oxide. Data in Figure 6 also indicated that at pH = 5.5 the capacity of As-adsorption follows the trend GSn5.5 > GSn2.1 > GSn0, confirming the possible use of GSn5.5 as a good adsorber for As removal technologies.

4. CONCLUSIONS

The following points are derived from the presented data.

- The preparation of Sn-goethites in basic media containing μ_{Sn} = 0.00, 5.00 and 10.00 mol mol^{-1}, and aged at 70° C for 20 days, renders metal deficient goethites with the following stoichiometry: α-$Fe_{0.948}O_{0.843}(OH)_{1.157}$ (GSn0), α-$Fe_{0.926}Sn_{0.020}O_{0.837}(OH)_{1.162}$ (GSn2.1) and α-$Fe_{0.920}Sn_{0.054}O_{0.921}(OH)_{1.0792}$ (GSn5.5).
- The Sn incorporation increases the thermal stability of the (hydr)oxides.
- The synthesized Sn-oxides present large mesoporous or even macropores, and the SSA followed the trend GSn5.5 > GSn0 > GSn2.1.
- The Sn-for-Fe substitution reduces the dissolution rate in acid media, and the most substituted sample is the most stable towards dissolution. Pure goethite dissolves more than two times faster than GSn5.5, and the trend in dissolution per unit area is GSn2.1 > GSn0 > GSn5.5, implying that a small degree of Sn-for-Fe substitution enhances the reactivity per unit area, and a larger degree of substitution passivate the surface towards mineral acid dissolution.

- The maximum of As(V) adsorption is found at pH 5.5 in all samples, where the monovalent As anion, $H_2AsO_4^-$, is the dominant species. After this maximum, the adsorption of As(V) decreases with the increase of pH in the range 6–11.
- The influence of pH on the adsorption of As is higher in the Sn-goethites than in the pure goethite, being the adsorption onto GSn5.5 the most affected by pH.
- The As(V) adsorption increases with the Sn content and the adsorption on sample GSn5.5 nearly duplicates the one showed by pure goethite.
- The high adsorption of As(V) on GSn5.5 and the low reactivity in acid solution of the oxide, when compared with pure goethite, imply that the Sn-α-FeOOH is a suitable candidate as an adsorbent in As(V) removal technologies.

5. ACKNOWLEDGMENTS

This research was supported by MINCYT through grant PICT 0780 (2008).

REFERENCES

[1] M.L. Pierce, C.B. Moore, Adsorption of arsenite and arsenate on amorphous iron hydroxide, Water Res. 16 (1982) 1247–1253.

[2] B.A. Manning, S. Goldberg, Modeling competitive adsorption of arsenate with phosphate and molybdate on oxide minerals, Soil Sci. Soc. Am. J. 60 (1996) 121–131.

[3] J. Aguilar, C. Dorronsoro, E. Fernández, J. Fernández, I. García, F. Martín, et al., Remediation of As-contaminated soils in the Guadiamar river basin (SW, Spain), Water. Air. Soil Pollut. 180 (2007) 109–118.

[4] R.M. Cornell, U. Schwertmann, The iron oxides: structure, properties, reactions, occurrences and uses, John Wiley & Sons, 2006.

[5] J.J. Wu, M. Muruganandham, J.S. Yang, S.S. Lin, Oxidation of DMSO on goethite catalyst in the presence of H2O2 at neutral pH, Catal. Commun. 7 (2006) 901–906.

[6] G.B. Ortiz de la Plata, O.M. Alfano, A.E. Cassano, Decomposition of 2-chlorophenol employing goethite as Fenton catalyst. I. Proposal of a feasible, combined reaction scheme of heterogeneous and homogeneous reactions, Appl. Catal. B Environ. 95 (2010) 1–13.

[7] G.B. Ortiz de la Plata, O.M. Alfano, A.E. Cassano, Decomposition of 2-chlorophenol employing goethite as Fenton catalyst II: Reaction kinetics of the heterogeneous Fenton and photo-Fenton mechanisms, Appl. Catal. B Environ. 95 (2010) 14–25.

[8] M. Muruganandham, J. Yang, J.J. Wu, Effect of Ultrasonic Irradiation on the Catalytic Activity and Stability of Goethite Catalyst in the Presence of H 2 O 2 at Acidic Medium, Ind. Eng. Chem. Res. 46 (2007) 691–698. doi:10.1021/ie060752n.

[9] B.C. Campo, O. Rosseler, M. Alvarez, E.H. Rueda, M.A. Volpe, On the nature of goethite, Mn-goethite and Co-goethite as supports for gold nanoparticles, Mater. Chem. Phys. 109 (2008) 448–454. doi:10.1016/j.matchemphys.2007.12.014.

[10] J. Lenz, B.C. Campo, M. Alvarez, M.A. Volpe, Liquid phase hydrogenation of α,β-unsaturated aldehydes over gold supported on iron oxides, J. Catal. 267 (2009) 50–56.

[11] D. Mohan, C.U. Pittman, Arsenic removal from water/wastewater using adsorbents-A critical review, J. Hazard. Mater. 142 (2007) 1–53. doi:10.1016/j.jhazmat.2007.01.006.

[12] Y. Masue, R.H. Loeppert, T.A. Kramer, Arsenate and arsenite adsorption and desorption behavior on coprecipitated aluminum: iron hydroxides, Environ. Sci. Technol. 41 (2007) 837–842.

[13] J. Silva, J.W. V Mello, M. Gasparon, W.A.P. Abrahão, V.S.T. Ciminelli, T. Jong, The role of Al-Goethites on arsenate mobility, Water Res. 44 (2010) 5684–5692.

[14] J. Gerth, Effects of crystal modification on the binding of trace metals and arsenate by goethite (7 pp), J. Soils Sediments. 5 (2005) 30–36.

[15] M. Mohapatra, S.K. Sahoo, S. Anand, R.P. Das, Removal of As (V) by Cu (II)-, Ni (II)-, or Co (II)-doped goethite samples, J. Colloid Interface Sci. 298 (2006) 6–12.

[16] B. Singh, D.M. Sherman, R.J. Gilkes, M.A. Wells, J.F.W. Mosselmans, Incorporation of Cr, Mn and Ni into goethite (α-FeOOH): mechanism from extended X-ray absorption fine structure spectroscopy, Clay Miner. 37 (2002) 639–649.

[17] M.A. Wells, R.W. Fitzpatrick, R.J. Gilkes, Thermal and mineral properties of Al-, Cr-, Mn-, Ni-and Ti-substituted goethite, Clays Clay Miner. 54 (2006) 176–194.

[18] S. Krehula, S. Musić, The influence of a Cr-dopant on the properties of α-FeOOH particles precipitated in highly alkaline media, J. Alloys Compd. 469 (2009) 336–342.

[19] E.E. Sileo, A.Y. Ramos, G.E. Magaz, M. a. Blesa, Long-range vs. short-range ordering in synthetic Cr-substituted goethites, Geochim. Cosmochim. Acta. 68 (2004) 3053–3063. doi:10.1016/j.gca.2004.01.017.

[20] M. Alvarez, E.E. Sileo, E.H. Rueda, Structure and reactivity of synthetic Co-substituted goethites, Am. Mineral. 93 (2008) 584–590. doi:10.2138/am.2008.2608.

[21] R. Pozas, T.C. Rojas, M. Ocaña, C.J. Serna, The nature of Co in synthetic Co-substituted goethites, Clays Clay Miner. 52 (2004) 760–766.

[22] U.G. Gasser, R. Nüesch, M.J. Singer, E. Jeanroy, Distribution of manganese in synthetic goethite, Clay Miner. 34 (1999) 291–299.

[23] E.E. Sileo, M. Alvarez, E.H. Rueda, Structural studies on the manganese for iron substitution in the synthetic goethite-jacobsite system, Int. J. Inorg. Mater. 3 (2001) 271–279.

[24] M. Alvarez, E.E. Sileo, E.H. Rueda, Effect of Mn (II) incorporation on the transformation of ferrihydrite to goethite, Chem. Geol. 216 (2005) 89–97.

[25] M. Alvarez, E.H. Rueda, E.E. Sileo, Structural characterization and chemical reactivity of synthetic Mn-goethites and hematites, Chem. Geol. 231 (2006) 288–299. doi:10.1016/j.chemgeo.2006.02.003.

[26] S. Krehula, S. Musić, Influence of Mn-dopant on the properties of α-FeOOH particles precipitated in highly alkaline media, J. Alloys Compd. 469 (2006) 327–334.

[27] E.E. Sileo, P.S. Solís, C.O. Paiva-Santos, Structural study of a series of synthetic goethites obtained in aqueous solutions containing cadmium (II) ions, Powder Diffr. 18 (2003) 50–55.

[28] M. Alvarez, M.F.M.F. Horst, E.E. Sileo, E.H. Rueda, Effect of Cd(II) on the ripening of ferrihydrite in alkaline

media, Clays Clay Miner. 60 (2012) 99–107. doi:10.1346/CCMN.2012.0600201.

[29] S. Krehula, S. Musić, The influence of Cd-dopant on the properties of α-FeOOH and α-Fe2O3 particles precipitated in highly alkaline media, J. Alloys Compd. 431 (2007) 56–64.

[30] N. Kaur, B. Singh, B.J. Kennedy, M. Gräfe, The preparation and characterization of vanadium-substituted goethite: The importance of temperature, Geochim. Cosmochim. Acta. 73 (2009) 582–593.

[31] N. Kaur, B. Singh, B.J. Kennedy, Copper substitution alone and in the presence of chromium, zinc, cadmium and lead in goethite (α-FeOOH), Clay Miner. 44 (2009) 293–310.

[32] N. Kaur, M. Gräfe, B. Singh, B. Kennedy, Simultaneous incorporation of Cr, Zn, Cd, and Pb in the goethite structure, Clays Clay Miner. 57 (2009) 234–250.

[33] N. Kaur, B. Singh, B.J. Kennedy, Dissolution of Cr, Zn, Cd, and Pb single-and multi-metal-substituted goethite: Relationship to structural, morphological, and dehydroxylation properties, Clays Clay Miner. 58 (2010) 415–430.

[34] B. Singh, M. Gräfe, N. Kaur, A. Liese, Applications of synchrotron-based X-ray diffraction and X-ray absorption spectroscopy to the understanding of poorly crystalline and metal-substituted iron oxides, Dev. Soil Sci. 34 (2010) 199–254.

[35] F.J. Berry, Ö. Helgason, A. Bohórquez, J.F. Marco, J. McManus, E.A. Moore, et al., Preparation and characterisation of tin-doped α-FeOOH (goethite), J. Mater. Chem. 10 (2000) 1643–1648. doi:10.1039/b0010561.

[36] A.L. Larralde, C.P. Ramos, B. Arcondo, A.E. Tufo, C. Saragovi, E.E. Sileo, Structural properties and hyperfine characterization of Sn-substituted goethites, Mater. Chem. Phys. 133 (2012) 735–740.

[37] D.G. Schulze, U. Schwertmann, G. Schulze, T.U. Mfinchen, W. Lafayette, The influence of aluminium on iron oxides: X. Properties of Al-substituted goethites, Clay Min. 19 (1984) 521–539.

[38] M.. Donohue, G.. Aranovich, Classification of Gibbs adsorption isotherms, Adv. Colloid Interface Sci. 76-77 (1998) 137–152. doi:10.1016/S0001-8686(98)00044-X.

[39] L. Daniel, N. Leonard, Spectrophotometric Study of the Bleaching of Ferric Thioglycolate, Contrib. from Dep. Chem. Lab. Nucl. Sci. Massachusetts Inst. Technol. 334 (1955) 552–556.

[40] V. Lenoble, V. Deluchat, B. Serpaud, J.-C. Bollinger, Arsenite oxidation and arsenate determination by the molybdene blue method, Talanta. 61 (2003) 267–276.

[41] K.S.W. Sing, Reporting physisorption data for gas/solid systems with special reference to the determination of surface area and porosity (Recommendations 1984), Pure Appl. Chem. 57 (1985) 603–619.

[42] T.J.W. De Bruijn, W.A. De Jong, P.J. Van Den Berg, Kinetic parameters in Avrami—Erofeev type reactions from isothermal and non-isothermal experiments, Thermochim. Acta. 45 (1981) 315–325.

[43] J.T. Carstensen, Stability of Solids and Solid Dosage Forms, J. Pharm. Sci. 63 (1974) 1–14.

[44] M.E. Brown, D. Dollimore, A.K. Galwey, Reactions in the solid state, Elsevier, 1980.

[45] A.E. Tufo, E.E. Sileo, P.J. Morando, Release of metals from synthetic Cr-goethites under acidic and reductive conditions: Effect of aging and composition, Appl. Clay Sci. 58 (2012) 88–95.

[46] P.R. Grossl, D.L. Sparks, Evaluation of contaminant ion adsorption/desorption on goethite using pressure jump relaxation kinetics, Geoderma. 67 (1995) 87–101.

[47] Y. Mamindy-Pajany, C. Hurel, N. Marmier, M. Roméo, Arsenic adsorption onto hematite and goethite, Comptes Rendus Chim. 12 (2009) 876–881.

[48] A. Garcia-Sanchez, E. Alvarez-Ayuso, F. Rodriguez-Martin, Sorption of As (V) by some oxyhydroxides and clay minerals. Application to its immobilization in two polluted mining soils, Clay Miner. 37 (2002) 187–194.

[49] Y.S. Ho, G. McKay, Pseudo-second order model for sorption processes, Process Biochem. 34 (1999) 451–465.

[50] M. Martínez, N. Miralles, S. Hidalgo, N. Fiol, I. Villaescusa, J. Poch, Removal of lead (II) and cadmium (II) from aqueous solutions using grape stalk waste, J. Hazard. Mater. 133 (2006) 203–211.

[51] V.C. Taty-Costodes, H. Fauduet, C. Porte, A. Delacroix, Removal of Cd (II) and Pb (II) ions, from aqueous solutions, by adsorption onto sawdust of Pinus sylvestris, J. Hazard. Mater. 105 (2003) 121–142.

[52] Y.S. Ho, W.T. Chiu, C. Sen Hsu, C.T. Huang, Sorption of lead ions from aqueous solution using tree fern as a sorbent, Hydrometallurgy. 73 (2004) 55–61.

[53] M. Arienzo, P. Adamo, J. Chiarenzelli, M.R. Bianco, A. De Martino, Retention of arsenic on hydrous ferric oxides generated by electrochemical peroxidation, Chemosphere. 48 (2002) 1009–1018. doi:10.1016/S0045-6535(02)00199-6.

[54] T. Hiemstra, Van Riemsdijk WH, Surface Structural Ion Adsorption Modeling of Competitive Binding of Oxyanions by Metal (Hydr)oxides., J. Colloid Interface Sci. 210 (1999) 182–193. doi:10.1006/jcis.1998.5904.

[55] D.M. Sherman, S.R. Randall, Surface complexation of arsenic(V) to iron(III) (hydr)oxides: Structural mechanism from ab initio molecular geometries and EXAFS spectroscopy, Geochim. Cosmochim. Acta. 67 (2003) 4223–4230. doi:10.1016/S0016-7037(03)00237-0.

[56] P. Lakshmipathiraj, B.R. V Narasimhan, S. Prabhakar, G. Bhaskar Raju, Adsorption of arsenate on synthetic goethite from aqueous solutions, J. Hazard. Mater. 136 (2006) 281–287. doi:10.1016/j.jhazmat.2005.12.015.

[57] J. Cervini-Silva, Coupled hydrophilic and charge-transfer interactions between polychlorinated methanes, ethanes, and ethenes and redox-manipulated smectite clay minerals, Langmuir. 20 (2004) 9878–9881. doi:10.1021/la0491089.

[58] Y. Gao, A. Mucci, Acid base reactions, phosphate and arsenate complexation, and their competitive adsorption at the surface of goethite in 0.7 M NaCl solution, Geochim. Cosmochim. Acta. 65 (2001) 2361–2378. doi:10.1016/S0016-7037(01)00589-0.

[59] J. Van Schuylenborgh, P.L. Arens, The Electrokinetic Behaviour Of Freshly Prepared g- and a-FeOOH, Recl. Des Trav. Chim. Des Pays-Bas. 69 (1950) 1557–1565.

[60] F. a. Vega, E.F. Covelo, M.L. Andrade, P. Marcet, Relationships between heavy metals content and soil properties in minesoils, Anal. Chim. Acta. 524 (2004) 141–150. doi:10.1016/j.aca.2004.06.073.